Modified Baryonic Dynamics: two-component cosmological simulations with light sterile neutrinos

JCAP10(2014)079

(http://iopscience.iop.org/1475-7516/2014/10/079)

Journal of Cosmology and Astroparticle Physics
An IOP and SISSA journal

Modified Baryonic Dynamics: two-component cosmological simulations with light sterile neutrinos

G.W. Angus,[a] **A. Diaferio,**[b,c,] **B. Famaey,**[d] **G. Gentile**[a,e] **and K.J. van der Heyden**[f]

[a]Department of Physics and Astrophysics, Vrije Universiteit Brussel, Pleinlaan 2, Brussels, 1050 Belgium
[b]Dipartimento di Fisica, Università di Torino, Via P. Giuria 1, Torino, I-10125 Italy
[c]Istituto Nazionale di Fisica Nucleare, Via P. Giuria 1, Torino, I-10125 Italy
[d]Observatoire astronomique de Strasbourg, CNRS UMR 7550, Université de Strasbourg, 11 rue de l'Université, Strasbourg, F-67000 France
[e]Sterrenkundig Observatorium, Universiteit Gent, Krijgslaan 281, Gent, 9000 Belgium
[f]Astrophysics, Cosmology & Gravity Centre, Dept. of Astronomy, University of Cape Town, Private Bag X3, Rondebosch, 7701 South Africa

E-mail: garry.angus@vub.ac.be, diaferio@ph.unito.it, benoit.famaey@astro.unistra.fr, gianfranco.gentile@ugent.be, heyden@ast.uct.ac.za

Received July 7, 2014
Revised September 3, 2014
Accepted October 8, 2014
Published October 30, 2014

JCAP10(2014)079

doi:10.1088/1475-7516/2014/10/079

Abstract. In this article we continue to test cosmological models centred on Modified Newtonian Dynamics (MOND) with light sterile neutrinos, which could in principle be a way to solve the fine-tuning problems of the standard model on galaxy scales while preserving successful predictions on larger scales. Due to previous failures of the simple MOND cosmological model, here we test a speculative model where the modified gravitational field is produced only by the baryons and the sterile neutrinos produce a purely Newtonian field (hence Modified Baryonic Dynamics). We use two-component cosmological simulations to separate the baryonic N-body particles from the sterile neutrino ones. The premise is to attenuate the over-production of massive galaxy cluster halos which were prevalent in the original MOND plus light sterile neutrinos scenario. Theoretical issues with such a formulation notwithstanding, the Modified Baryonic Dynamics model fails to produce the correct amplitude for the galaxy cluster mass function for any reasonable value of the primordial power spectrum normalisation.

Keywords: modified gravity, cosmological simulations, dark matter simulations, galaxy clusters

ArXiv ePrint: 1407.1207

JCAP10(2014)079

Contents

1 Introduction

Modified Newtonian Dynamics (MOND; [1], and see [2] for a recent review) is a modification to gravity in the ultra weak-field regime. It has a remarkable ability to reproduce the dynamics of galaxies of all types, shapes and sizes ([3–6]) — with only a few notable caveats ([7, 8]). On these scales, the standard cosmological model still struggles to reproduce the observed regularities in galaxy properties and has a number of other problems (see e.g. [9, 10]). On large scales, like clusters of galaxies, the MOND approach does not work [11–14]. There is a missing mass problem for MOND in clusters of galaxies. There is also no clear way to describe cosmological phenomena like the anisotropies in the cosmic microwave background (CMB; [15–18], but see [19]).

Approaching the missing mass problem from the other direction, cosmologists have found a satisfactory representation of the Universe at large scales using standard gravity (i.e. General Relativity). This comes through the combination of cold dark matter and dark energy (ΛCDM), with baryons making up a mere 5% of the energy budget. Invoking this combination allows the ΛCDM (or concordance) model to successfully match the acoustic peaks in the CMB [20]. Furthermore, the observed distribution of matter on large scales [21–23] is well reproduced by N-body simulations of structure formation [24–27]. Something that would confirm the ΛCDM model would be cosmological N-body simulations capable of producing galaxies that replicate the properties of observed galaxies ([9] and references therein). These observed properties of galaxies include the galaxy luminosity function [28–31], the relative frequencies of the various Hubble types [32], the colour bimodality [33–35], and — perhaps most importantly — dynamical properties elegantly encapsulated by MOND. Two of the most significant of these dynamical properties are (i) the baryonic Tully-Fisher relation [36, 37] and (ii) the scaling between the observed density profile of baryons and the inferred gravitational field (from a dynamical measure — [38]). This second property includes the requirement for dark matter (DM) to have a centrally cored distribution, rather than cusped [39, 40].

JCAP10(2014)079

Although there are promising efforts to satisfy the aforementioned criteria [40–45], these last two requirements remain illusive. The most common belief is that more sophisticated modelling of the complex hydrodynamical feedback processes, from central black holes and massive stars, will allow the observations and predictions to be reconciled [46–48].

Another approach is to assume MOND describes the dynamics of galaxies well and that we must blend a combination of MOND and DM together. An early attempt of this type came from [12] who added MOND and 2 eV active neutrinos together. This was not able to produce the measured acoustic peaks in the CMB, nor satisfy the requirement of DM in MOND clusters of galaxies [13, 49] due to phase space constraints. [50] suggested combining MOND with an 11 eV sterile neutrino, which was shown to be consistent with the CMB (under the ansatz that MOND is irrelevant at $z > 10^3$) and the phase-space constraints from clusters of galaxies [14]. The added attraction of this idea (which was reviewed by [51]) was that the 11 eV neutrinos would be fully thermalised, i.e. half of all quantum states would be occupied (just like the active neutrinos) — removing any fine tuning of their abundance. The other reason MOND plus sterile neutrinos is so attractive is that the free streaming properties of neutrinos on small scales means they would not influence galaxies. Thus, they would leave the impressive results of MOND in galaxies unblemished.

Using a purpose built MOND cosmological N-body code, [52] (hereafter AD11) showed this model was inconsistent with the observed cluster mass function — it produced too many high mass clusters and too few low mass clusters. [53] (hereafter A13) further demonstrated this behaviour for MOND cosmological simulations to produce too many superclusters was not limited to 11 eV sterile neutrinos. In fact, all masses of sterile neutrinos were ruled out, regardless of (i) the value of the MOND acceleration constant, (ii) the redshift at which MOND is "switched on", (iii) the normalisation of the initial conditions and (iv) the interpolating function. Other factors like the equation of state of dark energy were also shown to be ineffective.

In summary it does not appear to be possible to form the correct halo mass function in standard MOND from any sterile neutrino initial conditions that grew from an initially Harrison-Zel'dovich power spectrum under GR until $z \sim 200$. So if MOND is the correct description of gravitational dynamics on galaxy scales, then either the initial conditions are not as described above and yet conspire to produce the correct CMB angular power spectrum (a highly contrived scenario), or perhaps MOND does not affect the sterile neutrinos. This is important because although galaxies require MOND to form (and stably exist) without CDM, the clusters clearly do not require MOND at all and one should not ignore how well Newtonian gravity reproduces the cluster mass function.

At minimum, the ΛCDM model gives the correct cluster scale halo mass function at $z = 0$, whether some additional boost to gravity is required to form the clusters early enough has been discussed in the literature ([54–61]). MOND has a double negative effect on the cluster mass function if it influences the sterile neutrinos. Not only does it facilitate more rapid growth and the formation of much larger and denser structures than in Newtonian gravity, but these more massive halos now have MOND gravity meaning their dynamical masses are further enhanced, causing poorer agreement with the data. This result might suggest that if the MOND gravitational field is not produced by the sterile neutrinos (meaning only a Newtonian gravitational field is produced by them), but is only produced by the baryons, that it will have a positive influence on the halo mass function. Below we address how significant this influence is.

There is another factor to consider here which rules out the idea of MOND not being activated until some low redshift. That is that galaxies in MOND must form without the

JCAP10(2014)079

aid of a dark matter halo (cold, warm or hot) and galaxy formation without dark matter (if it is possible at all) is only possible with the added benefit of stronger than Newtonian gravitational attraction between the baryons. Thus, if MOND was not in effect until $z = 1$, then galaxies would not *begin* to form until then and galaxies are clearly formed long before this.

The simple options to blend MOND with DM are therefore ruled out. There are also more involved ideas, such as the tantalising theory of dipolar dark matter [62, 63] and bimetric MOND ([64, 65]), which require further investigation. However, a simpler framework may still exist with sterile neutrinos and MOND.

In the traditional framework of MOND, there exists no dark matter in galaxies. Therefore, it is assumed that only the baryons produce a modified gravitational field. In the extended frameworks, where MOND is blended with some species of neutrinos, it has always been assumed that the baryons and the neutrinos contribute to the modified gravitational field. On the other hand, there do exist modified theories of gravity (completely different to MOND) where the dark matter has a mutual fifth-force interaction, to which the baryons do not participate (e.g. [66, 67]). Here we go the other way, and suggest the baryons produce a modified gravitational field, but the sterile neutrinos do not. This can in principle retain all the benefits of adding sterile neutrinos to MOND — such as addressing the acoustic peaks of the CMB and solving the missing mass problem in MOND clusters. It also might evade the problems engendered when the sterile neutrinos produce a modified gravitational field — like overproducing massive clusters. Furthermore, in the original MOND + sterile neutrino framework, the effectiveness of MOND had to be "switched off" (i.e. the acceleration constant of MOND had to be substantially decreased) prior to recombination in an ad hoc way. This was to avoid MOND altering the shape of the CMB acoustic power spectrum. In a model where the sterile neutrinos do not produce a modified gravitational field, this would not be necessary.

In this article we run MOND cosmological simulations in a framework where the modified gravitational field is produced only by the baryons, not the sterile neutrinos. We present the framework and describe the simulation setup in section 2, show the results of our simulations in section 3 and in section 4 we give our conclusions.

2 Background and method

The Quasi-Linear formulation of MOND (QUMOND; [68]) requires solution of a modified version of the Poisson equation. Specifically, the ordinary Poisson equation for cosmological simulations

$$\nabla^2\Phi_N = 4\pi G(\rho - \bar{\rho})/a, \tag{2.1}$$

is solved to give the Newtonian potential, Φ_N, at scale factor a, from the ordinary matter density ρ that includes baryons and neutrinos. This would also include cold dark matter if there was any in our model. The QUMOND potential, Φ, is found from the Newtonian potential by solving

$$\nabla^2\Phi = \nabla\cdot[\nu(y)\nabla\Phi_N]\,, \tag{2.2}$$

and $y = \nabla\Phi_N/a_o a$, with a_o being the MOND acceleration constant chosen here to be $3.6\ (\mathrm{km\,s^{-1}})^2 pc^{-1}$. The interpolating ($\nu$) function is parametrised as per eqs. (51) and (53)

JCAP10(2014)079

of [2] where

$$\nu_\alpha(y) = \left[\frac{1+(1+4y^{-\alpha})^{1/2}}{2}\right]^{1/\alpha}, \tag{2.3}$$

and $\alpha = 1$ is the so-called simple ν-function and $\alpha = 2$ is the standard ν-function.

The specifics of how to solve eqs. (2.1) & (2.2) are explained in AD11 and further tests of the code were presented in A13.

The code written for AD11 and described therein is particle-mesh based, with a grid-mesh that has a limit of 257 cells in each dimension. In all our simulations we use 256 particles per dimension. Particle-mesh solvers are required to handle the non-linear MOND Poisson equation. Direct or tree-code methods fail because in MOND we cannot co-add particle gravities. The full MOND Poisson equation must be solved because the trivial MOND equation of spherical symmetry does not satisfy the conservation laws.

2.1 One-component simulations

Our original one-component simulations from AD11 and A13 use a single type of collisionless particle to represent the particle phase-space density of both DM and baryons, as is common in "DM only" N-body simulations. The simulations used in this article use a small modification to the original code to allow two-component simulations. That is, one species of collisionless particle represents the DM, and another (still collisionless) particle represents the baryons. Hereafter we describe the difference between the one-component and two-component simulations and how this facilitates our ability to test our hypothesis by generating different gravitational potentials from the DM and from the baryons.

Our one-component simulations are described by the following procedure:

- Particle positions and velocities are read in and the density of the particles is assigned to the various cells with the cubic cloud-in-cell method.
- Multi-grid methods (see Numerical Recipes §19.6) are used to solve the Poisson equation to find the Newtonian potential (eq. (2.1)). A 3D black-red sweep to update the cells with the new approximation of the potential in that cell and we iterate until we have fractional accuracy of 10^{-10}.
- The divergence of the vector in the square brackets of eq. (2.2) is taken which gives us the source of the QUMOND potential.
- The Poisson solving step is repeated, this time with the new source density to give the QUMOND potential, Φ, which we take the gradient of to find the gravity at each cell.
- Interpolate to each particle's position to find the appropriate gravity and move each particle with a second order leapfrog.
- The procedure repeats from the second stage until the simulation reaches $z = 0$.

2.2 Modified Baryonic Dynamics

The modification of gravity we propose is the following: the Newtonian potentials of the sterile neutrinos and baryons are found by solving the Newtonian Poisson equation

$$\begin{aligned} \nabla^2\Phi_{N,\nu_s} &= 4\pi G(\rho_{\nu_s} - \bar{\rho_{\nu_s}})/a \\ \nabla^2\Phi_{N,b} &= 4\pi G(\rho_b - \bar{\rho_b})/a. \end{aligned} \tag{2.4}$$

JCAP10(2014)079

The gravitational field produced by the sterile neutrinos is not modified and is thus $-\nabla\Phi_{N,\nu_s}$. On the other hand, the gravitational field produced by the baryons is found from the analogue of the QUMOND equation (eq. (2.2)), which is

$$\nabla^2\Phi_b = \nabla\cdot[\nu(y)\nabla\Phi_{N,b}]\,, \tag{2.5}$$

where crucially

$$y = \frac{|\nabla\Phi_{N,b} + \nabla\Phi_{N,\nu_s}|}{a_o a}. \tag{2.6}$$

The total modulus of the gravitational field experienced by any particle, sterile neutrino or baryon, is

$$\nabla\Phi = \nabla\Phi_{N,\nu_s} + \nabla\Phi_b. \tag{2.7}$$

Given that a modified gravitational field (relative to Newtonian gravity) is only produced by the baryons, we refer to this model as Modified Baryonic Dynamics (MBD).

From eq. (2.5) we see that the unmodified (Newtonian) gravitational field of the sterile neutrinos impacts the modification of the gravitational field of the baryons, due to its inclusion in the interpolating function ν. Therefore, the stronger the gravitational field of the sterile neutrinos (or the baryons independently) the weaker the modification to the baryonic gravitational field. However, the gravitational field of the sterile neutrinos is never modified. So all particles experience an unmodified Newtonian gravitational field generated by the sterile neutrinos, as well as a modified gravitational field generated by the baryons, where this very modification is influenced by the Newtonian gravitational field of the sterile neutrinos.

Note that, at this point, it is a phenomenological approach at the classical level: whether a Lagrangian producing these equations of motion can be found (both at the classical and covariant level) could be the subject of further work, if necessary. It is plausible that such a Lagrangian will require couplings of the baryons and sterile neutrinos to two different metrics, thereby leading to a violation of the weak-equivalence principle, which would have additional interesting consequences in their own right (see, e.g., [69]).

2.2.1 Initial conditions and simulation setup

In our one-component simulations (AD11 and A13) we made use of the original `COSMICS/GRAFICS` package of [70] to generate our initial conditions. We chose to input our own transfer functions using the massive neutrino parametrisation of [71] (their equations (10)–(12)) and the resulting linear matter power spectra were plotted for a sample of neutrino masses in A13 figure 1.

In order to exploit the MBD formulation we use the `GRAFICS-2` package of [72] which generates two sets of particles: baryons and sterile neutrinos (or any other DM particle one chooses), giving 256^3 for each species. The masses of the sterile neutrino and baryonic particles are found from $m = 1.4\times10^{11}\Omega_i(L_{\rm box}/N_p)^3 M_\odot$, where Ω_i should be replaced with either Ω_{ν_s} or Ω_b. It is then perfectly straight-forward to code the above expressions (eqs. (2.4)–(2.7)).

2.2.2 Two-component simulations

We then proceed as follows:

- Read in the positions of the sterile neutrinos, compute their density (ρ_{ν_s}) on the grid and then solve for their Newtonian potential (Φ_{N,ν_s}, as per eq. (2.4)) using finite differencing and multi-grid methods as described in AD11.

JCAP10(2014)079

- Read in the positions of the baryons, compute their density on the grid (ρ_b) and then their Newtonian potential ($\Phi_{N,b}$, as per eq. (2.4)).
- Derive $\nabla \cdot [\nu(y)\nabla\Phi_{N,b}]$, the QUMOND source density for the baryons, which uses eq. (2.6) as an argument for the interpolating function.
- Find the QUMOND potential for the baryons Φ_b, by solving eq. (2.5) using finite differencing.
- Add the QUMOND potential for the baryons together with the Newtonian potential for the sterile neutrinos (as in eq. (2.7)) to give the total potential, from which the gravitational field is derived to move both sets of particles.
- Interpolate to each particle's position to find the appropriate gravity and move each particle with a second order leapfrog.
- The procedure repeats from the second stage until the simulation reaches $z = 0$.

The clear difference between the one-component simulations and the two-component simulations is that in the latter the DM generates a Newtonian (not MONDian) gravitational field. As per A13, it is not possible to compare our two-component MBD simulations with a theoretical expectation because none exists. We can however run two-component simulations where we follow all the above steps but set $\nu = 1$. This, in effect, gives us a Newtonian simulation produced by the MBD machinery. In A13 we demonstrated that the one-component Newtonian simulations reproduced the theoretical halo mass function quite well. The two-component Newtonian simulations are indistinguishable from the one-component simulations, as expected. Unfortunately, there is no MOND or MBD theoretical mass function to compare with, but as can be seen in figure 1 of [5], the gravity solver in MOND works very well.

For the initial conditions, we employ the new CMB results provided by the PLANCK mission ([20]) which identifies (Ω_b, Ω_{ν_s}, Ω_Λ, h, n_s)=(0.049, 0.267, 0.683, 0.671, 0.962).

We use the quadrupole temperature, $Q_{\rm rms\text{-}PS}$, as a free parameter to fit the amplitude of the cluster mass function in MBD. The CMB quadrupole, $Q_{\rm rms\text{-}PS}$, is used to normalise the initial power spectrum of perturbations in the same way as σ_8 typically is for CDM simulations, because one cannot use linear theory in MOND to estimate σ_8 at $z = 0$.

3 Results

3.1 Newtonian equivalent mass

Using two-component simulations with sterile neutrinos, the baryons almost exactly trace the sterile neutrino distribution, which is not surprising. As with the original single component MOND simulations (A13), when computing the mass function to compare with observations, we use the Newtonian equivalent mass of halos — that is the dynamical mass our MOND halos would appear to have if probed using Newtonian dynamics. With MBD it is merely a case of separately running the AMIGA halo finder ([73, 74]) on both the baryons and sterile neutrinos (which gives identical halo numbers and halo particle mass distributions for our cluster sized halos). Then we calculate the Newtonian equivalent mass, $M_m(r) = M_b(r)\nu\left(\frac{GM_{\nu+b}(r)}{r^2 a_o}\right) + M_\nu(r)$, where the ν term only operates on the baryonic mass profile since the modification to gravity only affects the baryonic gravitational field. M_b and M_ν

JCAP10(2014)079

represent the particle mass profiles of baryons and sterile neutrinos respectively. From here we must find the radius where $M_m(r)$ encloses an average density of matter 200 times the critical density and build the mass function.

3.2 Renormalising the mass function

We ran 12 two-component simulations with different initial normalisations through the CMB quadrupole and different sterile neutrino masses. For each set of parameters, we ran two simulations: one with a 128 Mpc/h box and the other with a 256 Mpc/h box. We did this because we do not have adaptive mesh refinement built into our code, and it allows us to cover a larger range of masses in the halo mass function. Although the smaller boxes have higher spatial resolution, they have a limited halo mass range meaning poorer statistic i.e. the larger the box, the more massive the most massive halo it can form. However, in the simulations with the larger box, we have insufficient spatial resolution which leads to a suppression of the mass function.

The limited spatial resolution allows power on smaller scales to be leaked to larger scales. This can be seen clearly in figure 2 of A13 which plots the mass function using our simulations with Newtonian gravity and compares them with a theoretical mass function. For the 64 Mpc/h and 128 Mpc/h boxes, the simulations generally capture the correct amplitude of the theoretical mass function, except they under-predict for lower masses (smaller halos) and over-predict for larger masses (larger halos). For the 256 Mpc/h boxes, the amplitude of the theoretical mass function was generally under-predicted for all masses. Therefore, to use the 256 Mpc/h boxes (and thus probe out to slightly larger halo masses), we felt it was reasonable to increase the amplitude of their mass functions to agree with the amplitude of the 128 Mpc/h boxes. We use a single mass bin at $\log_{10}(M_{200}/M_\odot) = 14.2$ to make the renormalisation, but there would be very little difference if an average of many bins was used. The renormalisation predominantly results in an increase of 0.4 dex in the mass function amplitude, and one could equally well use this fixed value for the renormalisation. This makes little, if any, difference to the conclusions drawn in this article.

In figure 1 we plot the mass functions from simulations with the same neutrino mass of 100 eV, but various normalisations through the CMB quadrupole. The 128 Mpc/h box simulations extend from the left hand side of the plot until roughly $\log_{10}(M_{200}/M_\odot) = 14.3$. The 256 Mpc/h box simulations begin at roughly $\log_{10}(M_{200}/M_\odot) = 14.2$ and extend to the right hand side of the plot. The four normalisations used, in increasing amplitude, are $Q_{\text{rms-PS}} = 4$, 5, 9 and 17 μK (black, blue, red and green shaded curves respectively). Each shaded curve demonstrates the Poisson error. I.e. the top side of each shaded curve corresponds to the computed mass function plus the Poisson error. The under side corresponds to the computed mass function minus the Poisson error. We compare our simulated mass functions with data points from [21] (circles) and [22] (squares and triangles found using the virial theorem and the caustic technique respectively).

From figure 1 we see that $Q_{\text{rms-PS}} < 5\,\mu K$ is required to have a mass function amplitude which is comparable to the data (for a 100 eV sterile neutrino).

In general, the mass functions found using different normalisations, through the CMB quadrupole ($Q_{\text{rms-PS}}$), in pure MOND showed no variation (figure 7, A13) i.e. the mass functions had the same amplitude at $z = 0$ regardless of initial normalisation. The mass functions found with MBD clearly vary with normalisation.

In figure 2 we plot the mass functions from simulations with the same normalisation through the CMB quadrupole, of $Q_{\text{rms-PS}} = 4.5\,\mu K$, but three neutrino masses 50, 150 and

JCAP10(2014)079

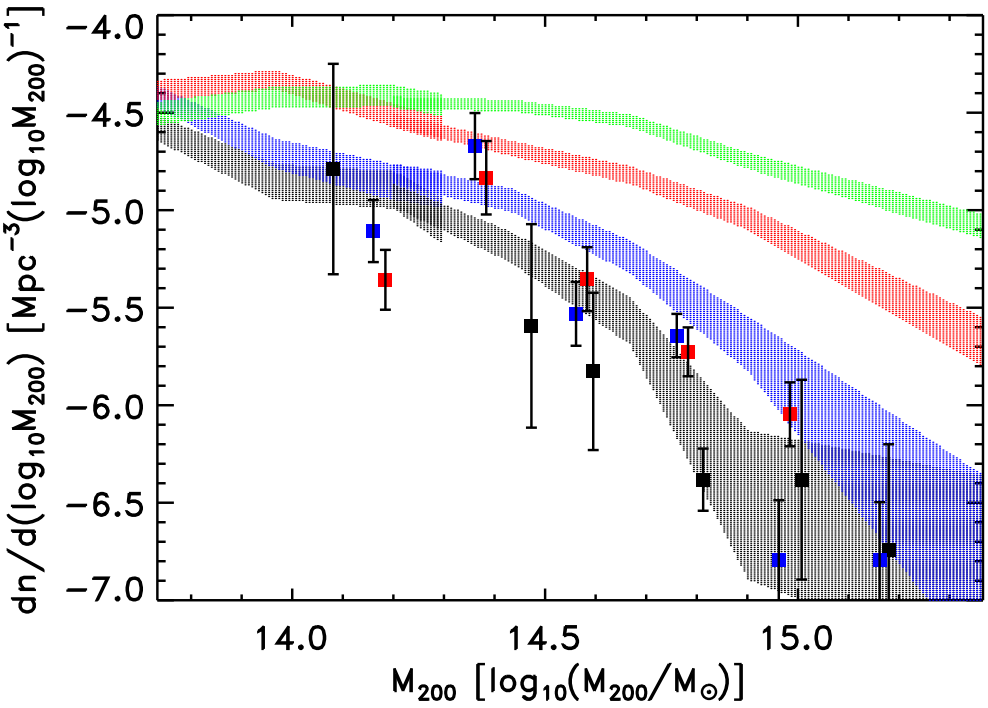

Figure 1. Plot of the mass functions from simulations with the same neutrino mass of 100 eV, but various normalisations through the CMB quadrupole. The 128 Mpc/h box simulations extend from the left hand side of the plot until roughly $\log_{10}(M_{200}/M_{\odot}) = 14.3$. The 256 Mpc/h box simulations begin at roughly $\log_{10}(M_{200}/M_{\odot}) = 14.2$ and extend to the right hand side of the plot. The four normalisations used, in increasing amplitude, are $Q_{\text{rms-PS}} = 4$, 5, 9 and 17 μK (black, blue, red and green shaded curves respectively). The top side of each shaded curve corresponds to the computed mass function plus the Poisson error. The under side corresponds to the computed mass function minus the Poisson error. The data points come from Reiprich & Böhringer (2002) (black squares) and Rines, Diaferio & Natarajan (2008) (blue and red squares found using the virial theorem and the caustic technique respectively).

JCAP10(2014)079

300 eV. We find that the lower the sterile neutrino mass, the lower the amplitude of the mass function and better the agreement with the observed cluster mass function. We only tested sterile neutrino masses between 50 and 300 eV, but using a mass of 30 eV or lower would not allow a fit to the cluster mass function. However, regardless of mass, a very low normalisation is always required.

To test if there was any sensitivity to the ν function (eq. (2.3)) employed, we ran two further MBD simulations using $\alpha = 2$ (the standard ν function), where the other MBD simulations used $\alpha = 1$ (the simple ν function). We chose $Q_{\text{rms-PS}} = 4.5$ and 12.5 μK and the result was that there is very little difference between simulations with $\alpha = 1$ and $\alpha = 2$. This means using any reasonable ν function in MBD will still require a low normalisation for the initial spectrum of perturbations, through the CMB quadrupole.

3.3 The significance of the CMB quadrupole

There are three values of the CMB quadrupole mentioned in this article. The measured one, the one fitted to the $l \gg 2$ CMB acoustic power spectrum and the one fitted to the mass function here (more often used in the form of σ_8 in ΛCDM papers).

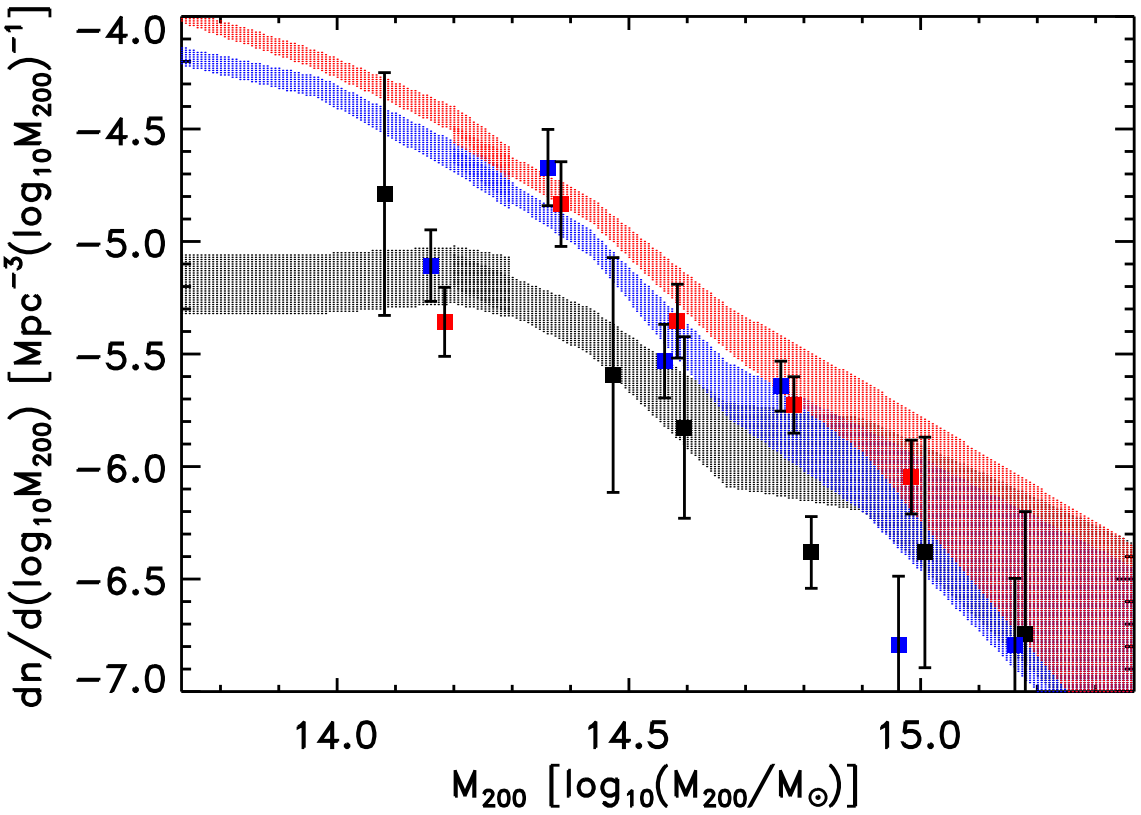

Figure 2. Plot showing the mass functions from Modified Baryonic Dynamics simulations with the same CMB quadrupole normalisation ($Q_{\text{rms-PS}} = 4.5\,\mu K$), but different sterile neutrino masses (starting from the bottom shaded curve): 50 (black), 150 (blue) and 300 eV (red). The 128 Mpc/h box simulations extend from the left hand side of the plot until roughly $\log_{10}(M_{200}/M_{\odot}) = 14.3$. The 256 Mpc/h box simulations begin at roughly $\log_{10}(M_{200}/M_{\odot}) = 14.2$ and extend to the right hand side of the plot. The top side of each shaded curve corresponds to the computed mass function plus the Poisson error. The under side corresponds to the computed mass function minus the Poisson error. The data points come from Reiprich & Böhringer (2002) (black squares) and Rines, Diaferio & Natarajan (2008) (blue and red squares found using the virial theorem and the caustic technique respectively).

The measured CMB quadrupole value is related to the multipole moment $l = 2$ coefficient, C_2^{TT}, as $Q_{\text{rms-PS}} = \left(\frac{5C_2^{TT}}{4\pi}\right)^{1/2}$. [75] and [76] plot likelihood versus quadrupole value in their figures 3 and 38 respectively. The allowed range at the one sigma level has shifted towards lower values in the latest paper and currently the lower one sigma confidence level is $C_2^{TT} \approx 50\,\mu K^2$ (the maximum likelihood is around $160\,\mu K^2$). This leads to $Q_{\text{rms-PS}} \approx 4.5\,\mu K$ at one sigma and roughly $8\,\mu K$ at maximum likelihood.

The fitted CMB quadrupole MBD requires to be consistent with the galaxy cluster mass function is $Q_{\text{rms-PS}} < 5\,\mu K$, which is roughly one sigma from the observed quadrupole.

In the ΛCDM model, a fitted quadrupole of around $21.5\,\mu K$ ([76]) is required so that the amplitude of the theoretical CMB power spectrum at multipoles $l \gg 2$ matches the observed spectrum. There should be consistency between the value of the quadrupole required to fit the CMB and other cosmological probes such as baryonic acoustic oscillations, galaxy clustering and the galaxy cluster mass function i.e. σ_8 should be the same for each probe. The fitted

JCAP10(2014)079

quadrupole to the CMB is generally consistent with most other probes of σ_8, but is between one and two sigma larger than the measured one. However, consistency with the measured one can be achieved by models that suppress the fitted one (due to inflationary theories, alternative gravity theories, etc) or increase the measured quadrupole (due to foreground modelling).

In the MBD case, we also expect the fitted quadrupole used to normalise the CMB ($21.4\,\mu K$ as per the ΛCDM value) and found from matching the galaxy cluster mass function to be the same. Clearly, the galaxy cluster mass function requires $Q_{\text{rms-PS}} < 5\,\mu K$ and the CMB requires $Q_{\text{rms-PS}} \approx 21.4\,\mu K$, so they are hugely discrepant. This is far more serious than a single, consistent fitted quadrupole (to the CMB and other probes) overestimating the measured one — as in the ΛCDM case.

4 Conclusion

In previous works (AD11 and A13) we tested the hypothesis that combining MOND with sterile neutrinos could produce the observed mass function of clusters of galaxies. We found it could not. This meant that, if MOND is the correct description of weak-field gravitational dynamics on galaxy scales, then either the whole cosmology and/or the initial conditions are not as described above (see, e.g., section 9.2 of [2] for a discussion in the context of covariant MOND theories), and yet would conspire to produce the correct CMB angular power spectrum (a highly contrived scenario), or perhaps MOND does not affect the sterile neutrinos in the same way as the baryons.

For this reason, we proposed that the modified gravitational field of MOND is only produced by the baryons. In this setup, the sterile neutrinos produce a Newtonian gravitational field. However, the baryons — subject to the total Newtonian gravitational field (both from the sterile neutrinos and baryons) — produce a MOND-like gravitational field.

There are similarities between our MBD model and many of the fifth force models referenced in [77]. For instance [67] employed a long range scalar field, generated only by the dark matter (not by the baryons), to increase the mutual acceleration of the two clusters comprising the colliding bullet cluster. In our MBD model, only the baryons generate a stronger than Newtonian gravitational attraction, whilst the sterile neutrinos produce a purely Newtonian gravitational field.

Our MBD model is far more conducive to producing a halo mass function that satisfies observational constraints than our previous attempts. Nevertheless, it requires fine tuning the normalisation of the primordial power spectrum, as is often done, through the CMB quadrupole, $Q_{\text{rms-PS}}$.

It was found that a normalisation of $Q_{\text{rms-PS}} < 5\,\mu K$ was required to have an adequate match and a lower sterile neutrino mass was preferred over a higher one.

The CMB quadrupole required is around 1 σ lower than the measured value from CMB observations ([76]). More significantly, this is much lower than the normalisation required to fit the CMB acoustic power spectrum in ΛCDM ($21.4\,\mu K$). This is crucial because we previously adopted the ΛCDM fits to the CMB as a basis for any MOND plus sterile neutrino theory, under the assumption the two models would give an identical CMB power spectrum.

We conclude therefore that the simple model considered here is not viable, and that more involved MOND models should be considered if the MOND phenomenology is indeed derived from a fundamental modification of the Lagrangian of Nature rather than an emergent phenomenon at galaxy scales. These theories must include at least one new degree of freedom

JCAP10(2014)079

corresponding to a non-trivial dark matter fluid with a non-trivial coupling to baryons. Interesting possibilities in this vein include dipolar dark matter [62, 63, 78] or BIMOND with twin matter [64, 65], as well as other possible frameworks still to be conceived.

Acknowledgments

GWA's research is supported by the FWO — Vlaanderen. AD acknowledges partial support from the INFN grant Indark and from the grant Progetti di Ateneo TO Call 2012 0011 'Marco Polo' of the University of Torino. The authors are grateful to the referee for valuable suggestions that significantly improved the content and readability of the paper.

References

[1] M. Milgrom, *A Modification of the Newtonian dynamics as a possible alternative to the hidden mass hypothesis*, *Astrophys. J.* **270** (1983) 365 [INSPIRE].

[2] B. Famaey and S.S. McGaugh, *Modified Newtonian Dynamics (MOND): Observational Phenomenology and Relativistic Extensions*, *Living Rev. Rel.* **15** (2012) 10 [arXiv:1112.3960] [INSPIRE].

[3] G. Gentile, B. Famaey and W.J.G. de Blok, *THINGS about MOND*, *Astron. Astrophys.* **527** (2011) A76 [arXiv:1011.4148] [INSPIRE].

[4] G.W. Angus, K.J. van der Heyden and A. Diaferio, *The dynamics of the bulge dominated galaxy NGC 7814 in MOND*, *Astron. Astrophys.* **543** (2012) A76 [arXiv:1303.0995] [INSPIRE].

[5] G.W. Angus, K.J. van der Heyden, B. Famaey, G. Gentile, S.S. McGaugh and W.J.G. de Blok, *A QUMOND galactic N-body code I: Poisson solver and rotation curve fitting*, *Mon. Not. Roy. Astron. Soc.* **421** (2012) 2598 [arXiv:1201.3185] [INSPIRE].

[6] R.H. Sanders, *A dearth of dark matter in strong gravitational lenses*, arXiv:1310.6148 [INSPIRE].

[7] G. Gentile et al., *HALOGAS: Extraplanar gas in NGC 3198*, *Astron. Astrophys.* **554** (2013) A125 [arXiv:1304.4232] [INSPIRE].

[8] G.W. Angus, G. Gentile, A. Diaferio, B. Famaey and K.J. van der Heyden, *N-body simulations of the Carina dSph in MOND*, *Mon. Not. Roy. Astron. Soc.* **440** (2014) 746 [arXiv:1403.4119] [INSPIRE].

[9] M.G. Walker and A. Loeb, *Is the Universe Simpler than ΛCDM?*, arXiv:1401.1146 [INSPIRE].

[10] P. Kroupa et al., *Local-Group tests of dark-matter Concordance Cosmology: Towards a new paradigm for structure formation?*, *Astron. Astrophys.* **523** (2010) A32 [arXiv:1006.1647] [INSPIRE].

[11] A. Aguirre, J. Schaye and E. Quataert, *Problems for MOND in clusters and the Lyα forest*, *Astrophys. J.* **561** (2001) 550 [astro-ph/0105184] [INSPIRE].

[12] R.H. Sanders, *Clusters of galaxies with modified Newtonian dynamics (MOND)*, *Mon. Not. Roy. Soc. Astron.* **342** (2003) 901 [astro-ph/0212293] [INSPIRE].

[13] G.W. Angus, B. Famaey and D.A. Buote, *X-ray Group and cluster mass profiles in MOND: Unexplained mass on the group scale*, *Mon. Not. Roy. Astron. Soc.* **387** (2008) 1470 [arXiv:0709.0108] [INSPIRE].

[14] G.W. Angus, B. Famaey and A. Diaferio, *Equilibrium configurations of 11 eV sterile neutrinos in MONDian galaxy clusters*, *Mon. Not. Roy. Astron. Soc.* **402** (2010) 395 [arXiv:0906.3322] [INSPIRE].

JCAP10(2014)079

[15] WMAP collaboration, D.N. Spergel et al., *Wilkinson Microwave Anisotropy Probe (WMAP) three year results: implications for cosmology*, *Astrophys. J. Suppl.* **170** (2007) 377 [astro-ph/0603449] [INSPIRE].

[16] WMAP collaboration, E. Komatsu et al., *Seven-Year Wilkinson Microwave Anisotropy Probe (WMAP) Observations: Cosmological Interpretation*, *Astrophys. J. Suppl.* **192** (2011) 18 [arXiv:1001.4538] [INSPIRE].

[17] WMAP collaboration, G. Hinshaw et al., *Nine-Year Wilkinson Microwave Anisotropy Probe (WMAP) Observations: Cosmological Parameter Results*, *Astrophys. J. Suppl.* **208** (2013) 19 [arXiv:1212.5226] [INSPIRE].

[18] Atacama Cosmology Telescope collaboration, J.L. Sievers et al., *The Atacama Cosmology Telescope: Cosmological parameters from three seasons of data*, *JCAP* **10** (2013) 060 [arXiv:1301.0824] [INSPIRE].

[19] C. Skordis, D.F. Mota, P.G. Ferreira and C. Bœhm, *Large Scale Structure in Bekenstein's theory of relativistic Modified Newtonian Dynamics*, *Phys. Rev. Lett.* **96** (2006) 011301 [astro-ph/0505519] [INSPIRE].

[20] Planck collaboration, P.A.R. Ade et al., *Planck 2013 results. XVI. Cosmological parameters*, accepted in *Astron. Astrophys.* (2014) [arXiv:1303.5076] [INSPIRE].

[21] T.H. Reiprich and H. Böhringer, *The Mass function of an X-ray flux-limited sample of galaxy clusters*, *Astrophys. J.* **567** (2002) 716 [astro-ph/0111285] [INSPIRE].

[22] K. Rines, A. Diaferio and P. Natarajan, *WMAP5 and the Cluster Mass Function*, *Astrophys. J.* **679** (2008) L1 [arXiv:0803.1843] [INSPIRE].

[23] A. Vikhlinin et al., *Chandra Cluster Cosmology Project III: Cosmological Parameter Constraints*, *Astrophys. J.* **692** (2009) 1060 [arXiv:0812.2720] [INSPIRE].

[24] W.H. Press and P. Schechter, *Formation of galaxies and clusters of galaxies by selfsimilar gravitational condensation*, *Astrophys. J.* **187** (1974) 425 [INSPIRE].

[25] J.M. Bardeen, J.R. Bond, N. Kaiser and A.S. Szalay, *The Statistics of Peaks of Gaussian Random Fields*, *Astrophys. J.* **304** (1986) 15 [INSPIRE].

[26] J.R. Bond, S. Cole, G. Efstathiou and N. Kaiser, *Excursion set mass functions for hierarchical Gaussian fluctuations*, *Astrophys. J.* **379** (1991) 440 [INSPIRE].

[27] R.K. Sheth and G. Tormen, *An Excursion set model of hierarchical clustering: Ellipsoidal collapse and the moving barrier*, *Mon. Not. Roy. Astron. Soc.* **329** (2002) 61 [astro-ph/0105113] [INSPIRE].

[28] P. Schechter, *An analytic expression for the luminosity function for galaxies*, *Astrophys. J.* **203** (1976) 297 [INSPIRE].

[29] 2dFGRS collaboration, S. Cole et al., *The 2dF Galaxy Redshift Survey: Near infrared galaxy luminosity functions*, *Mon. Not. Roy. Astron. Soc.* **326** (2001) 255 [astro-ph/0012429] [INSPIRE].

[30] E.F. Bell, D.H. McIntosh, N. Katz and M.D. Weinberg, *The optical and near-infrared properties of galaxies. 1. Luminosity and stellar mass functions*, *Astrophys. J. Suppl.* **149** (2003) 289 [astro-ph/0302543] [INSPIRE].

[31] SDSS collaboration, M.R. Blanton et al., *The Galaxy luminosity function and luminosity density at redshift $z = 0.1$*, *Astrophys. J.* **592** (2003) 819 [astro-ph/0210215] [INSPIRE].

[32] L.S. Kelvin, S.P. Driver, A.S.G. Robotham, A.W. Graham, S. Phillipps et al., *Galaxy And Mass Assembly (GAMA): ugrizYJHK Sérsic luminosity functions and the cosmic spectral energy distribution by Hubble type*, arXiv:1401.1817 [INSPIRE].

JCAP10(2014)079

[33] I.K. Baldry et al., *Quantifying the bimodal color-magnitude distribution of galaxies*, *Astrophys. J.* **600** (2004) 681 [astro-ph/0309710] [INSPIRE].

[34] M.L. Balogh, I.K. Baldry, R. Nichol, C. Miller, R. Bower and K. Glazebrook, *The Bimodal galaxy color distribution: Dependence on luminosity and environment*, *Astrophys. J.* **615** (2004) L101 [astro-ph/0406266] [INSPIRE].

[35] S.P. Driver et al., *The millennium galaxy catalogue: morphological classification and bimodality in the colour-concentration plane*, *Mon. Not. Roy. Astron. Soc.* **368** (2006) 414 [astro-ph/0602240] [INSPIRE].

[36] S.S. McGaugh, J.M. Schombert, G.D. Bothun and W.J.G. de Blok, *The Baryonic Tully-Fisher relation*, *Astrophys. J.* **533** (2000) L99 [astro-ph/0003001] [INSPIRE].

[37] S.S. McGaugh, *The Baryonic Tully-Fisher relation of galaxies with extended rotation curves and the stellar mass of rotating galaxies*, *Astrophys. J.* **632** (2005) 859 [astro-ph/0506750] [INSPIRE].

[38] S.S. McGaugh, *The balance of dark and luminous mass in rotating galaxies*, *Phys. Rev. Lett.* **95** (2005) 171302 [astro-ph/0509305] [INSPIRE].

[39] G. Gentile, P. Salucci, U. Klein, D. Vergani and P. Kalberla, *The Cored distribution of dark matter in spiral galaxies*, *Mon. Not. Roy. Astron. Soc.* **351** (2004) 903 [astro-ph/0403154] [INSPIRE].

[40] F. Governato et al., *At the heart of the matter: the origin of bulgeless dwarf galaxies and Dark Matter cores*, *Nature* **463** (2010) 203 [arXiv:0911.2237] [INSPIRE].

[41] F. Governato et al., *Forming disk galaxies in ΛCDM simulations*, *Mon. Not. Roy. Astron. Soc.* **374** (2007) 1479 [astro-ph/0602351] [INSPIRE].

[42] F. Governato et al., *Forming a Large Disk Galaxy from a $z < 1$ Major Merger*, *Mon. Not. Roy. Astron. Soc.* **398** (2009) 312 [arXiv:0812.0379] [INSPIRE].

[43] A.A. Dutton, *The baryonic Tully-Fisher relation and galactic outflows*, *Mon. Not. Roy. Astron. Soc.* **424** (2012) 3123 [arXiv:1206.1855] [INSPIRE].

[44] G.S. Stinson, C. Brook, A.V. Macciò, J. Wadsley, T.R. Quinn and H.M.P. Couchman, *Making Galaxies in a Cosmological Context: The Need for Early Stellar Feedback*, *Mon. Not. Roy. Astron. Soc.* **428** (2013) 129 [arXiv:1208.0002] [INSPIRE].

[45] G.S. Stinson et al., *MaGICC Thick Disk I: Comparing a Simulated Disk Formed with Stellar Feedback to the Milky Way*, *Mon. Not. Roy. Astron. Soc.* **436** (2013) 625 [arXiv:1301.5318] [INSPIRE].

[46] D. Sijacki, M. Vogelsberger, D. Kereš, V. Springel and L. Hernquist, *Moving mesh cosmology: the hydrodynamics of galaxy formation*, *Mon. Not. Roy. Astron. Soc.* **424** (2012) 2999 [arXiv:1109.3468] [INSPIRE].

[47] M. Vogelsberger, S. Genel, D. Sijacki, P. Torrey, V. Springel and L. Hernquist, *A model for cosmological simulations of galaxy formation physics*, *Mon. Not. Roy. Astron. Soc.* **436** (2013) 3031 [arXiv:1305.2913] [INSPIRE].

[48] AGORA collaboration, J.-h. Kim et al., *The AGORA High-Resolution Galaxy Simulations Comparison Project*, *Astrophys. J. Suppl.* **210** (2014) 14 [arXiv:1308.2669] [INSPIRE].

[49] G.W. Angus, H.Y. Shan, H.S. Zhao and B. Famaey, *On the Law of Gravity, the Mass of Neutrinos and the Proof of Dark Matter*, *Astrophys. J.* **654** (2007) L13 [astro-ph/0609125] [INSPIRE].

[50] G.W. Angus, *Is an 11 eV sterile neutrino consistent with clusters, the cosmic microwave background and modified Newtonian dynamics?*, *Mon. Not. Roy. Astron. Soc.* **394** (2009) 527.

JCAP10(2014)079

[51] A. Diaferio and G.W. Angus, *The Acceleration Scale, Modified Newtonian Dynamics and Sterile Neutrinos*, arXiv:1206.6231 [INSPIRE].

[52] G.W. Angus and A. Diaferio, *The abundance of galaxy clusters in MOND: Cosmological simulations with massive neutrinos*, *Mon. Not. Roy. Astron. Soc.* **417** (2011) 941 [arXiv:1104.5040] [INSPIRE].

[53] G.W. Angus, A. Diaferio, B. Famaey and K.J. van der Heyden, *Cosmological simulations in MOND: the cluster scale halo mass function with light sterile neutrinos*, *Mon. Not. Roy. Astron. Soc.* **436** (2013) 202 [arXiv:1309.6094] [INSPIRE].

[54] C.R. Mullis et al., *Discovery of an X-ray-luminous galaxy cluster at $z = 1.4$*, *Astrophys. J.* **623** (2005) L85 [astro-ph/0503004] [INSPIRE].

[55] M.N. Bremer et al., *XMM-LSS discovery of a $z = 1.22$ galaxy cluster*, *Mon. Not. Roy. Astron. Soc.* **371** (2006) 1427 [astro-ph/0607425] [INSPIRE].

[56] M.J. Jee et al., *Hubble Space Telescope Weak-lensing Study of the Galaxy Cluster XMMU J2235.3-2557 at $Z \sim 1.4$: A Surprisingly Massive Galaxy Cluster when the Universe is One-third of its Current Age*, *Astrophys. J.* **704** (2009) 672 [arXiv:0908.3897] [INSPIRE].

[57] M.J. Jee et al., *Scaling Relations and Overabundance of Massive Clusters at $z \gtrsim 1$ from Weak-Lensing Studies with HST*, *Astrophys. J.* **737** (2011) 59 [arXiv:1105.3186] [INSPIRE].

[58] P. Rosati et al., *Multi-wavelength study of XMMU J2235.3-2557: the most massive galaxy cluster at $z > 1$*, *Astron. Astrophys.* **508** (2009) 583 [arXiv:0910.1716] [INSPIRE].

[59] M. Brodwin et al., *SPT-CL J0546-5345: A Massive $Z > 1$ Galaxy Cluster Selected Via the Sunyaev-Zel'dovich Effect with the South Pole Telescope*, *Astrophys. J.* **721** (2010) 90 [arXiv:1006.5639] [INSPIRE].

[60] M. Brodwin et al., *IDCS J1426.5+3508: Sunyaev-Zel'dovich Measurement of a Massive IR-selected Cluster at $Z = 1.75$*, *Astrophys. J.* **753** (2012) 162 [arXiv:1205.3787] [INSPIRE].

[61] R.J. Foley et al., *Discovery and Cosmological Implications of SPT-CL J2106-5844, the Most Massive Known Cluster at $z > 1$*, *Astrophys. J.* **731** (2011) 86 [arXiv:1101.1286] [INSPIRE].

[62] L. Blanchet and A.L. Tiec, *Model of Dark Matter and Dark Energy Based on Gravitational Polarization*, *Phys. Rev.* **D 78** (2008) 024031 [arXiv:0804.3518] [INSPIRE].

[63] L. Blanchet and A.L. Tiec, *Dipolar Dark Matter and Dark Energy*, *Phys. Rev.* **D 80** (2009) 023524 [arXiv:0901.3114] [INSPIRE].

[64] M. Milgrom, *Matter and twin matter in bimetric MOND*, *Mon. Not. Roy. Astron. Soc.* **405** (2010) 1129 [arXiv:1001.4444] [INSPIRE].

[65] M. Milgrom, *MOND and its bimetric formulation*, arXiv:1310.3373 [INSPIRE].

[66] A. Nusser, S.S. Gubser and P.J.E. Peebles, *Structure formation with a long-range scalar dark matter interaction*, *Phys. Rev.* **D 71** (2005) 083505 [astro-ph/0412586] [INSPIRE].

[67] G.R. Farrar and R.A. Rosen, *A New Force in the Dark Sector?*, *Phys. Rev. Lett.* **98** (2007) 171302 [astro-ph/0610298] [INSPIRE].

[68] M. Milgrom, *Quasi-linear formulation of MOND*, *Mon. Not. Roy. Astron. Soc.* **403** (2010) 886 [arXiv:0911.5464] [INSPIRE].

[69] J.-M. Alimi and A. Füzfa, *The Abnormally Weighting Energy Hypothesis: the Missing Link between Dark Matter and Dark Energy*, *JCAP* **09** (2008) 014 [arXiv:0804.4100] [INSPIRE].

[70] E. Bertschinger, *COSMICS: cosmological initial conditions and microwave anisotropy codes*, astro-ph/9506070 [INSPIRE].

[71] K. Abazajian, *Linear cosmological structure limits on warm dark matter*, *Phys. Rev.* **D 73** (2006) 063513 [astro-ph/0512631] [INSPIRE].

JCAP10(2014)079

[72] E. Bertschinger, *Multiscale Gaussian random fields for cosmological simulations*, *Astrophys. J. Suppl.* **137** (2001) 1 [astro-ph/0103301] [INSPIRE].

[73] S.P.D. Gill, A. Knebe and B.K. Gibson, *The Evolution substructure 1: A New identification method*, *Mon. Not. Roy. Astron. Soc.* **351** (2004) 399 [astro-ph/0404258] [INSPIRE].

[74] S.R. Knollmann and A. Knebe, *AHF: AMIGA's Halo Finder*, *Astrophys. J. Suppl.* **182** (2009) 608 [arXiv:0904.3662] [INSPIRE].

[75] C.L. Bennett et al., *Seven-Year Wilkinson Microwave Anisotropy Probe (WMAP) Observations: Are There Cosmic Microwave Background Anomalies?*, *Astrophys. J. Suppl.* **192** (2011) 17 [arXiv:1001.4758] [INSPIRE].

[76] WMAP collaboration, C.L. Bennett et al., *Nine-Year Wilkinson Microwave Anisotropy Probe (WMAP) Observations: Final Maps and Results*, *Astrophys. J. Suppl.* **208** (2013) 20 [arXiv:1212.5225] [INSPIRE].

[77] P.J.E. Peebles and A. Nusser, *Clues from nearby galaxies to a better theory of cosmic evolution*, *Nature* **465** (2010) 565 [arXiv:1001.1484] [INSPIRE].

[78] L. Blanchet and L. Bernard, *Phenomenology of MOND and gravitational polarization*, *Int. J. Mod. Phys. Conf. Ser.* **30** (2014) 1460271 [arXiv:1403.5963] [INSPIRE].

JCAP10(2014)079